Palaeogeography, Palaeoclimatology, Palaeoecology 409 (2014) 239–248

Contents lists available at ScienceDirect

Palaeogeography, Palaeoclimatology, Palaeoecology

journal homepage: www.elsevier.com/locate/palaeo

Varied responses of forest at its distribution margin to Holocene monsoon development in northern China

Qian Hao, Hongyan Liu *, Yi Yin, Hongya Wang, Mingmin Feng

College of Urban and Environmental Sciences and MOE Laboratory for Earth Surface Processes, Peking University, Beijing, 100871, China

ARTICLE INFO

Article history:
Received 30 November 2013
Received in revised form 17 May 2014
Accepted 20 May 2014
Available online 24 May 2014

Keywords:
Palaeovegetation
Forest-steppe ecotone
Monsoon
Drought
Holocene

ABSTRACT

Based on pollen analysis and other evidence in a sediment profile from Huangqihai Lake, located at the limit of Asian monsoon influence, the local vegetation development and climatic change were reconstructed for the past 8600 years. From 8600 to 7200 cal. yr BP, the local vegetation was dominated by steppe and tree cover was low. Then pine increased gradually, and the local vegetation was pine and oak mixed forest with variable ratios of the two dominant tree taxa from 7200 to 3600 cal. yr BP. From 3600 to 3000 cal. yr BP, the forest was replaced by shrubland, which was attributed to a period of intense drought. From 3000 to 600 cal. yr BP, the tree cover declined to its lowest levels, probably due to long-term further drought. After 600 cal. yr BP, steppe has become dominant again. We found that the changes of vegetation type indicated by pollen percentages did not match existing evidence for monsoon dynamics. Changes in tree pollen concentration, however, well captured the changes in the Asian monsoon, implying different sensitivity of vegetation cover and vegetation type (e.g. replacement of steppe by forest) to the monsoon development. In addition, a shrubland-dominated stage which has not been evident in previous studies was also clear in our pollen sequences. Our study implied that the responses of marginal forest to drought were variable, depending on the drought regime. The different responses of forest to climate drying in this study provide insights into the reliable prediction of forest dynamics in the semi-arid regions.

1. Introduction

Drought has a significant influence on forest decline, as shown by recently increasing drought-induced tree mortality at the edges of the forest distribution all over the world (Adams et al., 2009; Van Mantgem et al., 2009; Allen et al., 2010; Qiu, 2010; Peng et al., 2011). As a result of forest decline, three kinds of vegetation dynamics have been observed under different climatic conditions: replacement of forest by grassland, savannification, and shrubland expansion (Calvao and Palmeirim, 2004; Acácio et al., 2009; Frelich and Reich, 2009). In order to reliably predict which kind of vegetation dynamics will occur under future climate drying, we need to reconstruct past forest dynamics at the edge of the current forest distribution, using palynological evidence.

The monsoon climate determines forest distribution in the eastern part of China, with the limit of the monsoon influence lying close to the 400 mm mean annual precipitation (MAP) isohyet. This isohyet divides the semi-arid and semi-humid regions as well as the forest and steppe vegetation. Local-scale forest and steppe are mosaic and patch distributed, with shrubland separating them locally at the edge of the monsoon's influence (Liu et al., 2012). Palynological works in this region have mainly focused on changes in vegetation types, particularly the replacement of forest by steppe during the Holocene, through interpretation of pollen percentage sequences (Xiao et al., 2004; Jiang et al., 2006; Chen et al., 2008; Wang et al., 2010; Yin et al., 2011). Although a few studies have considered changes in pollen percentages, they have failed to link these with regional vegetation cover and climatic change. The Holocene climatic change in this region was characterized by both a long-term drying trend and severe drought events (Zhao et al., 2009; Yin et al., 2013). We propose the hypothesis that different kinds of responses, for example savannification and shrubland expansion, in addition to replacement of forest by steppe, might have occurred during the Holocene as responses to different drought regimes.

We chose Huangqihai Lake, located in the forest-steppe ecotone in northern China, to reconstruct the changes in vegetation and climate during the Holocene. In this paper, based on well-dated high-resolution lake sediment records, we present the vegetation history in the Huangqihai Lake region, including the dynamics of both vegetation type and tree cover, during the past 8600 cal. yr BP. With independent drought proxies obtained from lake sediments, we particularly focus on how vegetation development has responded to drought in this study.

* Corresponding author.
E-mail address: lhy@urban.pku.edu.cn (H. Liu).

http://dx.doi.org/10.1016/j.palaeo.2014.05.020
0031-0182/

2. Material and Methods

2.1. Study area

Huangqihai Lake (40°41′–41°43′ N, 112°49′–113°40′ E) is situated in the central part of Inner Mongolia, China, with a maximum water surface area of 110 km^2, a maximum length of 20 km and a maximum width of 9 km. About 19 rivers flow into Huangqihai, including Bawang River and Quyuanlin River (Zhang et al., 2011). Because of climatic change and human water use, Huangqihai Lake is desiccated seasonally or all year round (Zhang et al., 2011) (Fig. 1).

Located at the transition between the semi-humid and semi-arid areas in the temperate zone of China (Zhang et al., 2011), the mean annual temperature (MAT) is 4.5 °C and MAP is about 360 mm in the Huangqihai region. The climate is mainly controlled by the Siberian-Mongolian high-pressure system in winter, resulting in cold and dry

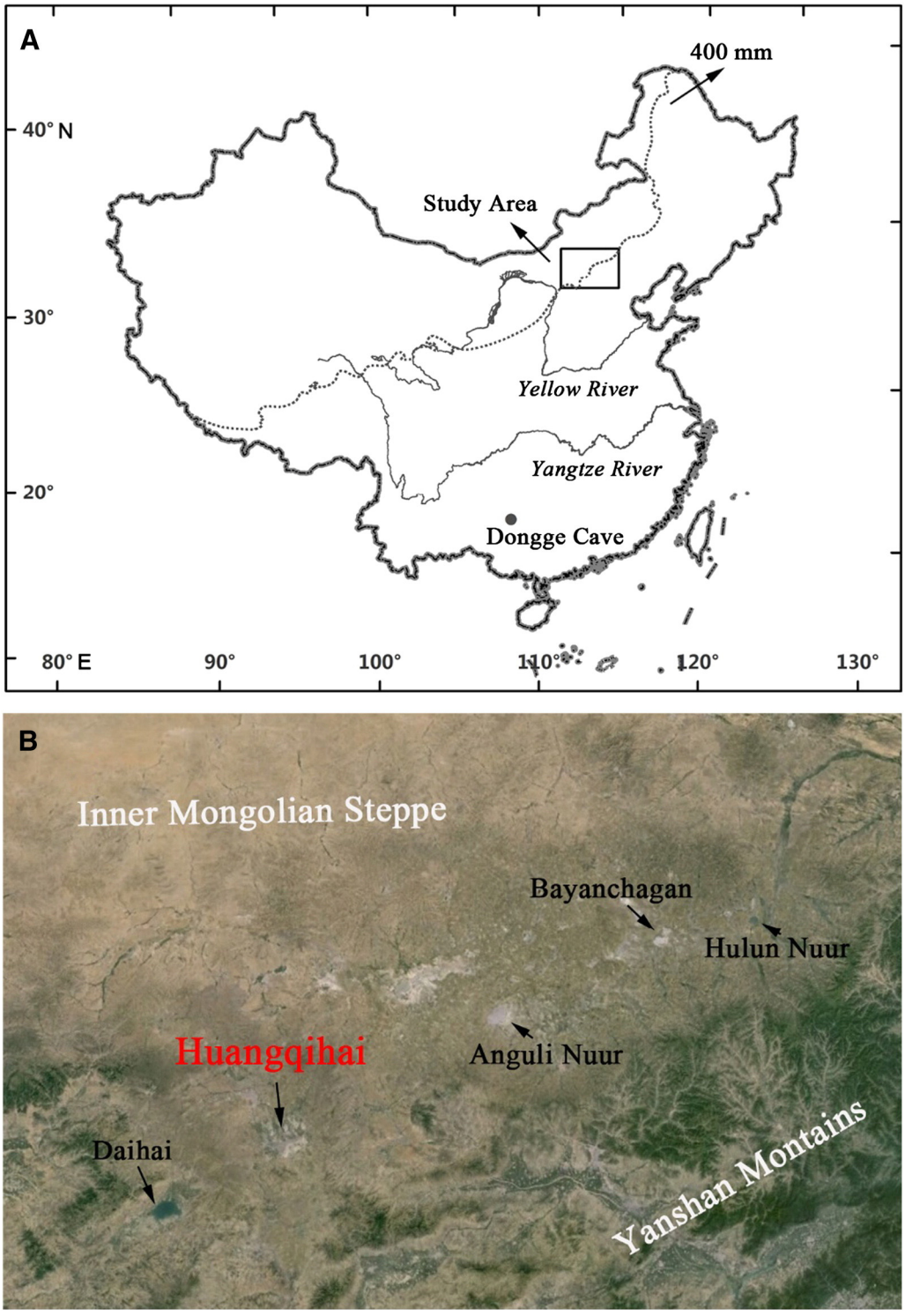

Fig. 1. Location of Lake Huangqihai at regional and local scales. (A) Map of China showing location of study region, Dongge Cave and 400 mm isohyet (rectangle area as shown in detail in B); (B) Satellite image of the study area showing the study site (Huangqihai Lake) and other sites discussed in the text, including Daihai, Anguli Nuur, Bayanchagan and Hulun Nuur.

environmental conditions. Warm temperatures and high humidity are brought by the prevailing Asian monsoon in summer. Approximately 66% of the annual precipitation falls from June to August (Zhang et al., 2011). The mean annual evaporation is 1930 mm (Zhang et al., 2011).

The regional vegetation around the lake in the Huangqihai Lake is temperate steppe dominated by *Stipa krylovii* (Wu, 1980). On the surrounding mountains, the common tree taxa are *Pinus tabulaeformis*, *Picea meyeri*, *Populus davidiana, Betula phatyphylla, Ulmus pumila* and *Salix* spp.. The ground flora include *Spiraea* spp., *Hippophae rhamnoides*, *Ostryopsis davidiana*, *Prunus armeniaca*, *Lespedaza bicolor*, *Carex* spp., *Artemisia* spp. and *Chenopodium acuminatum*.

We used previously reported pollen or other sediment proxies from four lakes close to Huangqihai Lake in order to compare the local and regional vegetation similarities and differences. Hulun Nuur, which is also located in the semi-arid region, has a surface water area about 5 times greater than Huangqihai Lake. Bayanchagan is close to the Otindag Sandy Plain, 180 km northwest of Huangqihai Lake. Anguli Nuur is located between Bayanchagan and Huangqihai. Daihai Lake is located in the 55 km southwest of Huangqihai. These lakes are all located at the margin of the monsoon influence and the MAP of these sites is between 350 and 450 mm. They have similar present-day vegetation types and patterns (Fig. 1).

2.2. Sediment coring and chronology

An 820 cm core (location 40°50′ N, 113°17′ E) was recovered in January 2012 with a UWITEC piston corer made in Austria (Fig. 1B). The upper 70 cm was collected by digging a section and the remaining 750 cm was drilled. The location of the core was selected to avoid direct inflow influences, to ensure continuous deposition of the lake sediments. The core was packed and transferred to the laboratory at Peking University, then resampled at 1-cm intervals and dried in the laboratory.

Fifteen samples were selected according to lithological transition and depth, and AMS ^{14}C dating was performed in the AMS Laboratory of Peking University. All dates were calibrated to calendar years before present (cal. yr BP) with the Callib611 programme, using the IntCal04 calibration data set (Reimer et al., 2004) (Fig. 2). Four abnormal values with evident age reversal were rejected and one sample did not meet the test quality requirement. As a result, 10 chronological data were used to establish a piecewise linear fitting in the Huangqihai Lake core analysis (Table 1).

In the lake sediment environment, the reservoir effect is frequently the important factor affecting the chronology accuracy (Ren, 1998; An et al., 2012). Using the dated age of 1444 cal yr BP at the depth of 3 cm and 2851 cal yr BP at the depth of 67 cm, the age of the lake surface (0 cm) was extrapolated to an age of 1378 cal. yr BP. Given the age of lake surface (0 cm) was the year of coring (2012 A.D.), we suggested a possible reservoir effect of 1440 years (sum of 1378 years and the difference between 2012 and 1950 that BP is defined).

The whole core was divided into 4 sections based on the changes in lithology and deposition rate. The sediment mainly consists of sandy silt with brown–gray color above 67 cm and the grain becomes fine with green–gray color between 67 and 103 cm. During the depth of 103 to 770 cm, the color is green–black fine-grained clayey silt. In the deepest portion, it contained medium-grained silt with brown–gray color (Fig. 2). The ages of each sampling interval above 103 cm or below 770 cm of the core were established by linear interpolation using the adjacent two corrected calendar age dates or by extrapolation beyond the oldest dated level. The ages between the 103 and 770 cm samples were established by an age-depth model based on 7 corrected calendar age dates, which revealed a linear relationship ($r^2 = 0.98$) between core depth and age (Fig. 2).

2.3. Pollen analysis and data interpretation

Sediment samples were analyzed every 5 cm. A total of 164 samples were collected for pollen analysis. For each sample of 4–8 cm^3 sediments, 30% hydrochloric acid (HCl) was added and the sample was left for 18 h to remove carbonates, then boiled in 10% sodium hydroxide (NaOH) for 30 min to remove organic matter. Next, the samples were sieved though 180 μm and 7 μm sieves and treated with a heavy liquid solution (KI + HI + Zn) with a specific gravity of about 2.0 to extract

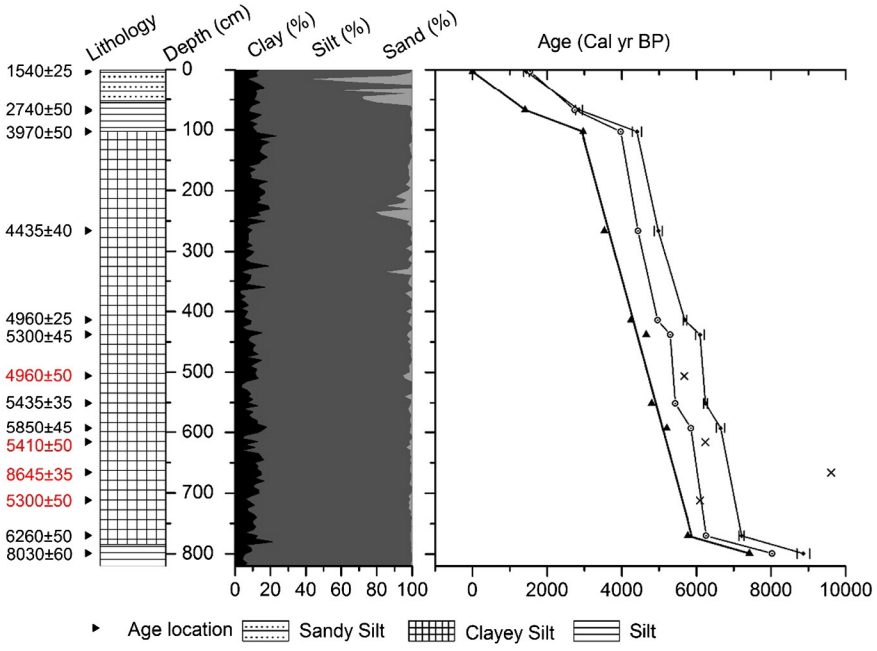

Fig. 2. Age–depth curve of the Lake Huangqihai sediment core. Circles represent radiocarbon dates, diamonds represent calibrated radiocarbon dates with vertical bars showing the date range (2δ), triangles represent corrected calendar age dates, and crosses represent abnormal values. The grain-size distribution with depth is shown in the middle. Lithological changes are shown on the left.

Table 1
AMS radiocarbon dates and calibrated years of samples from the Huangqihai sediment core.

Laboratory number	Depth in core (cm)	Dating material	^{14}C age (yr BP)	Calibrated ^{14}C age(2δ) (cal. yr BP)	Corrected calendar age (cal. yr BP)
BA12653	3	Bulk sediment	1540 ± 25	1370 ~ 1519 (1444)	66
BA12654	68	Bulk sediment	NA		
BA12655	67	Bulk sediment	2740 ± 50	2757 ~ 2946 (2851)	1473
BA12656	103	Bulk sediment	3970 ± 50	4281 ~ 4534 (4407)	3029
BA12657	266	Bulk sediment	4435 ± 40	4873 ~ 5079 (4976)	3598
BA12658	414	Bulk sediment	4960 ± 25	5641 ~ 5739 (5690)	4312
BA12659	438	Bulk sediment	5300 ± 45	5984 ~ 6206 (6095)	4717
BA12660	506	Bulk sediment	4960 ± 50	5594 ~ 5758 (5676)	4298
BA12661	551	Bulk sediment	5435 ± 35	6187 ~ 6296 (6241)	4863
BA12662	592	Bulk sediment	5850 ± 45	6535 ~ 6757 (6646)	5268
BA12663	616	Bulk sediment	5410 ± 50	6172 ~ 6300 (6236)	4858
BA12664	666	Bulk sediment	8645 ± 35	9539 ~ 9678 (9608)	8230
BA12665	712	Bulk sediment	5300 ± 50	5981 ~ 6208 (6094)	4716
BA12666	770	Bulk sediment	6260 ± 50	7142 ~ 7276 (7209)	5831
BA12667	799	Bulk sediment	8030 ± 60	8691 ~ 9032 (8861)	7483

pollen from sediments (http://www.ucl.ac.uk/GeolSci/micropal/spore.html). Finally, the extracted samples were treated by acetolysis (Moore et al., 1991).

A tablet of *Lycopodium* spores (about 27,637 grains) was added to each of the samples as exotic markers, thus the pollen concentration could be obtained (Maher and Louis, 1981). Pollen taxa were identified under an Olympus optical microscope at 400× magnification, and more than 200 terrestrial pollen grains were counted for each sample (Liu et al., 2010).

Pollen percentages of the main taxa, the ratio of *Artemisia* to Chenopodiaceae (A/C), the ratio of arboreal plants to non-arboreal plants (AP/NAP), and the pollen concentration of all taxa are presented. The A/C ratio has been used as a good indicator of available moisture in arid and semi-arid regions because *Artemisia* and Chenopodiaceae indicate steppe- and desert-dominated vegetation, respectively (Herzschuh, 2007; Zhao et al., 2007; Huang et al., 2009; Zhao et al., 2012). Recent work showed that the A/C ratio has a positive relationship with moisture in areas with MAP less than 450–500 mm (Zhao et al., 2012). AP/NAP was better than A/C for indicating available moisture in forest regions with MAP higher than 450–500 mm, with higher values indicating higher available moisture (An et al., 2006).

2.4. Physical and chemical analyses of sediment and data interpretation

2.4.1. Grain size

Approximately 0.3–0.4 g of each sample was used for grain size measurement by Malvern Mastersizer 2000. Before the measurement, 10–20 ml of 30% H_2O_2 was added until no more bubbles formed, to remove organic matter. Then the samples were boiled with enough 10% HCl to remove carbonates. Deionized water was used to rinse acidic ions until the pH value was close to 7. Finally, samples were boiled with 10 ml 0.5 mol/L $(NaPO_3)_6$. Within 3 h, these samples were treated on an ultrasonic vibrator for 30 s and the grain distribution was divided into 3 classes, clay (<2 μm), silt (2–63 μm) and sand (>63 μm).

In general, the sand percentage indicated wind strength in the arid region (De Deckker et al., 1991; Porter and An, 1995; Qiang et al., 2007) while it indicated hydrological activity in humid region (Wu et al., 2006). In the semi-arid region, it represented both wind and water activity intensity. While the precipitation was relatively low and the evaporation was high, most precipitation was evaporated, resulting in weak runoff. At the same time, because of the small difference in elevation across the basin and the disc shape of lake, it was hard for runoff to carry sand to the lake center directly. Also, the intense wind activity, poor vegetation coverage and long freeze-up period led to coarse particles being moved into the center of the lake by the wind (Zhai et al., 2006). Therefore, the sand carried to lake center was mostly brought into the lake center by wind rather than by water, and therefore the percentage of coarse particles indicated winter wind activity in a dry and cold climate (Yin et al., 2011).

2.4.2. Total organic carbon (TOC) and Total Nitrogen (TN)

After removing the roots and other macro-organic remains, and grinding to pass through a 149 μm soil sieve, total carbon (TC) and total nitrogen (TN) were measured by an Elementar Vario EL (Germany). In order to get the total organic carbon (TOC) values, we firstly measured the amount of total inorganic carbon (TIC) by adding enough HCl into the sediment samples with measured weight. By measuring the volume of CO_2 produced, the amount of total inorganic carbon (TIC) was calculated. Then TOC was achieved by subtracting TIC from TC.

When the climate was warm and humid, the forest generally grew better than the grasses, and the value of C/N was higher. Besides, hydrological activities were stronger when precipitation was higher, and more terrestrial soil material would have therefore been brought to the basin, resulting in a higher C/N value (O'Reilly et al., 2003). At the same time, the lake level change could have caused sediment disturbance, promoting the decomposition of organic matter (Kernan et al., 2010). While the climate was humid, the disturbance was low, generating high C/N values. In summary, C/N (TOC/TN) could be used as an indicator of climate, with a higher C/N indicating a warm and humid environment and a lower C/N suggesting a dry and cold environment (Rosén and Hammarlund, 2007; Williams et al., 2009). In addition, a higher TOC value alone was suggested to indicate a warmer and more humid climate (Rosén, 2005), and in particular higher precipitation, in the semi-arid region of China (Xiao et al., 2006).

2.4.3. Loss on ignition (LOI)

LOI was measured by the weight difference of about 1 g sediment sample before and after it was placed into the Muffle furnace and baked at 980 °C for 30 min. LOI reflected both organic matter and $CaCO_3$ content, which in general coincided with the fine grain-size and TOC value.

3. Results

3.1. Pollen assemblages in Huangqihai Lake

Over 30 families and genera of pollen were identified in samples of Huangqihai core sediments (Fig. 3). These included major tree taxa such as *Pinus, Picea, Abies, Quercus, Betula, Ulmus, Alnus* and *Tilia*, major shrub taxa such as *Corylus, Ostryopsis* and *Ephedra*, and major herbs of *Artemisia*, Chenopodiaceae, Poaceae, Cyperaceae, *Polygonum*, Rosaceae, Ranunculaceae, Lamiaceae, Farbaceae and Asteraceae. According to the

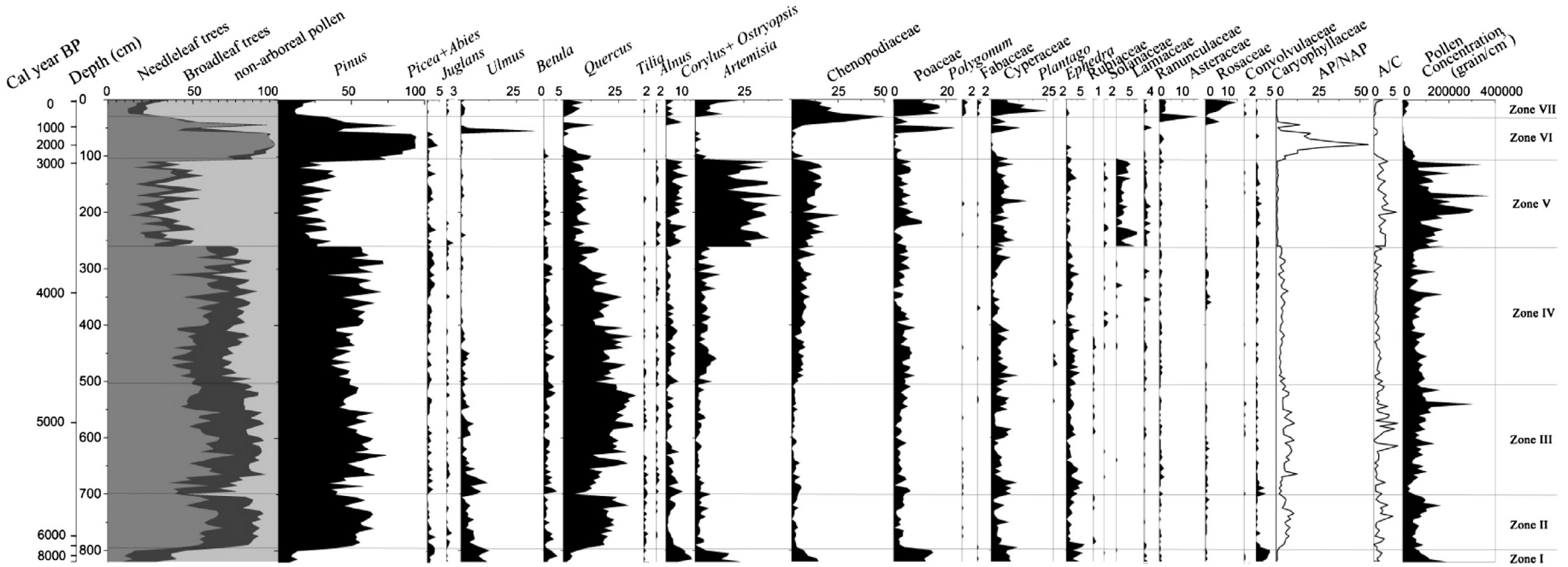

Fig. 3. Pollen percentage diagram, with pollen density of all taxa and pollen zones of the Huangqihai Lake. The A/C and AP/NAP values are also shown in the diagram.

differences in pollen assemblage and concentration at different depths, the pollen diagrams were divided into 7 zones.

3.1.1. Zone I (820–795 cm, 8620 to 7190 cal. yr BP)

Pinus was at its lowest percentage of the whole sequence, while the *Ulmus* and *Corylus* (and *Ostryopsis*) had relative high values. Herb pollens were present at high percentages, especially the *Artemisia*, Chenopodiaceae, Poaceae, Cyperaceae and *Ephedra*. Over all, tree pollen percentages were low while steppe pollen percentages were relatively high.

It is inferred from the pollen assemblage that steppe dominated, and was associated with shrubs at this stage. Broadleaved tree pollen and pine pollen might have been transported into this lake from a distance, because scattered trees or forests existed in this area. Pollen concentration was not low through the whole sequence, indicating a high vegetation cover in the steppe.

3.1.2. Zone II (795–700 cm, 7190 to 5550 cal. yr BP)

Pinus pollen exceeded 50% and became a dominant component in this zone, and *Quercus* accounted for higher than 15% of total pollen, resulting in a consistently high AP content (~85%). In contrast, percentages of the pollen of *Artemisia*, Chenopodiaceae and other herb pollen percentages remained at low levels. The A/C ratio was higher than that in zone I. In this zone, *Pinus* and *Quercus* mixed forest replaced the steppe.

3.1.3. Zone III (700–505 cm, 5550 to 4700 cal. yr BP)

The pollen assemblages were dominated by *Pinus* (higher than 50%). This zone showed a continuous increase of *Quercus* (from 5% to 27%), while other broadleaf trees pollen percentages decreased gradually. Compared with the last stage, herb taxa pollen percentages changed only slightly. The pollen concentrations and percentages of broadleaved tree species increased remarkably and the total pollen concentration also increased, indicating high vegetation cover.

3.1.4. Zone IV (505–260 cm, 4700 to 3640 cal. yr BP)

The pollen value of *Quercus* dropped markedly from 25% to 10%. There were a small increase of *Artemisia* and Chenopodiaceae pollen percentage and a small decline in the A/C mean ratio. However, *Pinus* and other herb pollen percentages remained stable during this period. These results indicated that vegetation previously dominated by broadleaved trees was gradually replaced by conifer woodlands.

3.1.5. Zone V (260–105 cm, 3640 to 2970 cal. yr BP)

The arboreal pollen percentage decreased, while *Artemisia* and Chenopodiaceae pollen percentages increased markedly to 25% and 20% respectively, with additional increases in other herb pollen values. In addition, the A/C ratio increased and was generally >2. The pollen percentages of shrub species, including *Corylus* and *Ostryopsis*, also showed substantial increases. This zone was again characterized by relatively high pollen concentrations, reaching a maximum of 380,000 grains/cm^3. This indicated a high vegetation cover, while the tree cover did not increase. Therefore, shrub and herb species increased markedly, while the coniferous forest was replaced by shrublands.

3.1.6. Zone VI (105–30 cm, 2970to 600 cal. yr BP)

Pinus dominated the pollen assemblages (more than 90%), while other kinds of pollen contributed little to the total pollen. Thus, the AP/NAP ratio was extremely high (up to 50). The pollen concentration reduced to its lowest value in the sequence, indicating that the site vegetation coverage was extremely low. Pine pollen, which had low concentrations, likely came from surrounding regions.

3.1.7. Zone VII (30–0 cm, 600 cal. yr BP to present)

The pollen assemblages were dominated by herbaceous taxa, especially Chenopodiaceae, Poaceae, Cyperaceae and *Ephedra*. Percentages of Chenopodiaceae pollen increased and reached a maximum of 25%. The A/C ratio was low (<1 in most cases). In addition, there were great fluctuations in almost all the pollen taxa. Although the tree taxa increased in the latter part of this zone, the area was still dominated by drought-tolerant species of the steppe landscape.

3.2. LOI, TOC/TN and Grain-size

From 8620 to about 7200 cal. yr BP, the sand percentage was relatively stable (Fig. 4). The values of TOC and TN clearly increased, but the C/N and LOI remained low compared with the following stage. This indicated a relatively dry and cold climate. From about 7200 to 4700 cal. yr BP, the percentage of sand still remained very low, even close to 0, while the clay fraction increased slightly. Overall, the C/N and LOI values showed a little growth, suggesting a higher precipitation than that during the previous stage. These indexes were consistent with the change of pollen described above. The average sand/non-sand ratio increased during 4700 to 3500 cal. yr BP while the LOI value remained stable. The C/N value rose slightly, while the TOC value declined. Thus, the climate was becoming dry and cold during this period. There was a significant change during the period of about 3500 to 1300 cal. yr BP. While C/N reached its maximum value of the whole study period, TOC, TN and LOI values dropped substantially. Thus, the climate might have become colder and drier compared with that in the previous stage. During the last 1300 cal. yr BP, the most remarkable change was in the value of sand/non-sand, which reached its maximum of all the stages. The C/N fell to its lowest value. The TOC and TN increased in the latter part of the stage. These trends indicated a cold and dry climate, which became warmer and wetter later (about 600 cal. yr BP) in the stage.

4. Discussion

4.1. Holocene climatic change at the limit of monsoon influence

Our results confirmed the effects of the Asian monsoon on regional climate because our results for grain size percentage and TOC in general well captured the monsoon dynamics (Fig. 5). Stalagmite ^{18}O isotopes, which have the advantages of continuous preservation and accurate dating, have been widely used as proxies for the Asian monsoon intensity (Cai et al., 2001; Fleitmann et al., 2003, 2007; Dykoski et al., 2005; Hu et al., 2008; Wu et al., 2011). Though many studies suggested that stalagmite ^{18}O isotopes in southern China may not indicate the intensity of Asian Monsoon or precipitation (Maher, 2008; Clemens et al., 2010; Pausata et al., 2011), it was found significantly correlate with the rainfall in northern China by modelling and experiments (Liu et al., 2014). Stalagmite ^{18}O isotope curve from Dongge Cave in southern China (Dykoski et al., 2005) shows that the Asian Monsoon remained strong during 10 to 6 cal. ka BP, while at 6 to 5 cal. ka BP, the monsoon began to weaken significantly, indicating decreasing rainfall. This phenomenon continued until 1 cal. ka BP (Dykoski et al., 2005). Our TOC value showed a similar trend and clearly decreased after 4700 cal. yr BP. During the most recent 600 years, the monsoon influence increased slightly but remained low. The TOC value also increased slightly and the sand percentage grew (Fig. 5). Other evidence such as sand dune fixation in the early to middle Holocene and activation in the late Holocene in Inner Mongolia of China also roughly followed the monsoon-dominated climate change in our study region (Fig. 5. Sun et al., 2006; Zhou et al., 2008).

However, there were also some details in our climatic proxies that were inconsistent with the monsoon dynamics. There existed discrepancy between TOC and LOI during 8 to 6 cal. ka BP (Fig. 4). LOI was measured using the Muffle furnace and the temperature was 980 °C in this research which was sufficiently high to remove all organic and inorganic matters. This might account for the inconsistency between the LOI and TOC values during 9 to 6 cal. yr BP. During 7 to 6 cal. ka BP, the TOC

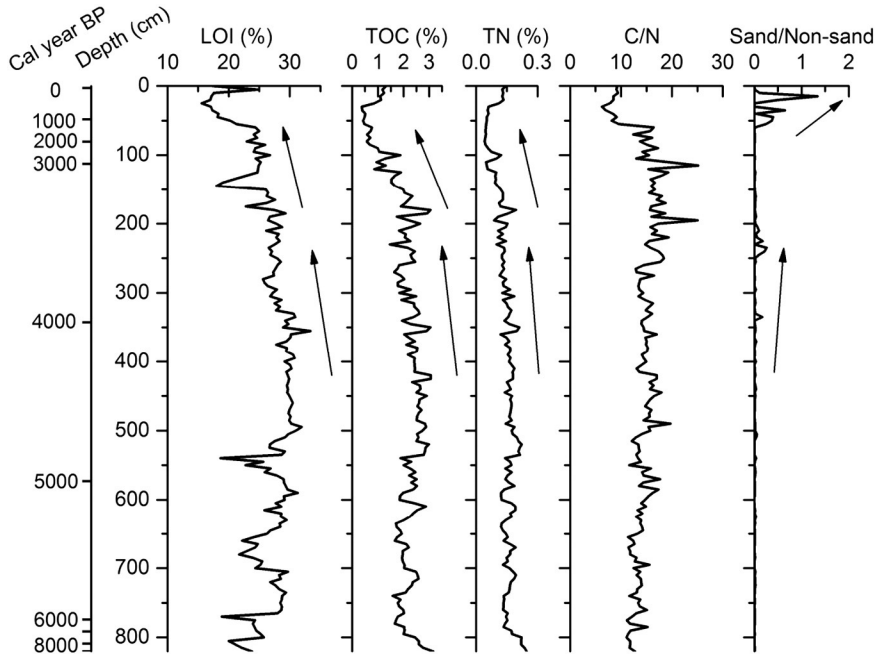

Fig. 4. Changes in loss on ignition (LOI), total organic carbon (TOC) content, total nitrogen (TN) content, TOC/TN and the ratio of sand to non-sand particles (silt and clay).

value was relatively low while the monsoon intensity remained high (Fig. 5). In a previous study in Huangqihai, the Rb/Sr and magnetic susceptibility values that could be used as a surrogate of summer monsoon intensity indicated a warmer and wetter climate, which was consistent with the monsoon changes rather than our TOC trend (Shen et al., 2006). The fixation of sand dunes also indicated a wetter climate (Sun et al., 2006; Zhou et al., 2008; Yang et al., 2010). Percentages of sand at both Huangqihai in our study and at Anguli Nuur (Yin et al., 2011) remained relatively low during this stage and were consistent with the monsoon change. However, the C/N values from Daihai were relatively low, similarly to our result. The inconsistency between TOC (or C/N) and other proxies could be attributed to the low-resolution of TOC sampling (only 4 values) during this period in our results (Fig. 5). Another reason could be that the TOC or C/N value not only reflected the vegetation type changes but also the ratio of terrestrial plants to aquatic plants (Battarbee, 2010).

The mid- to late-Holocene dry period is an almost undisputed event at regional scale despite the inconsistencies described above. At local scale, the Rb/Sr ratio seemed to well match the regional drying trend, but data are not available for the recent 2000 years (Shen et al., 2006;

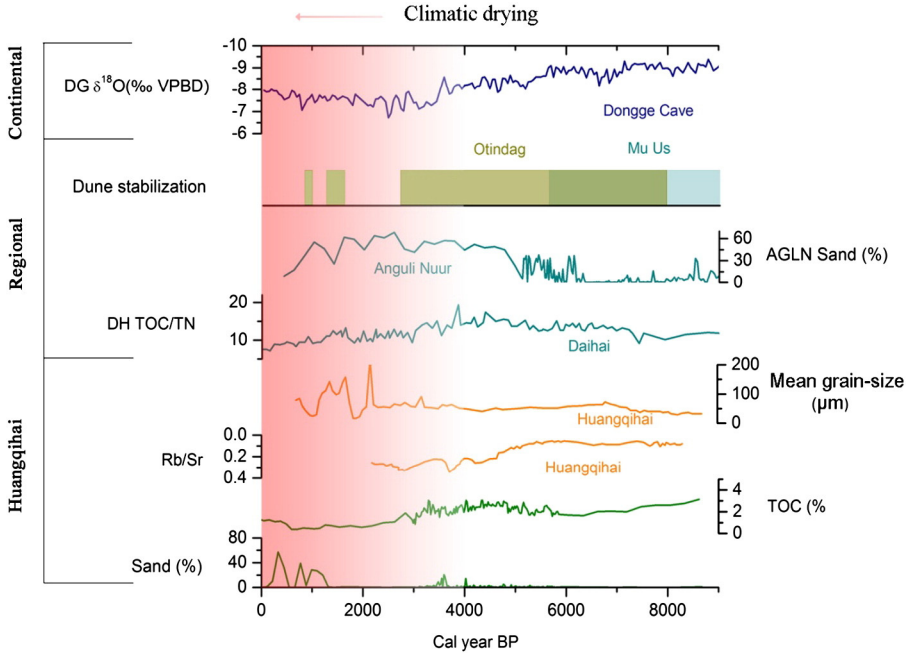

Fig. 5. Proxies of climate evolution on different spatial scales. Continental scale: precipitation change during the Holocene, based on stalagmite ^{18}O isotopes of Dongge (DG) (Dykoski et al., 2005); Regional scale: physical or chemical indexes including sand dune activity of Otindag and Mu Us Sandy Lands, sand percentage of Anguli Nuur (AGLN) and TOC/TN value of Daihai (DH) (Sun et al., 2006; Xiao et al., 2006; Zhou et al., 2008; Liu et al., 2010; Yang et al., 2010); Local scale: physical or chemical indexes at Huangqihai in our study and previous studies, including TOC percentage (this study), sand percentage (this study), soil mean grain-size and Rb/Sr value (Shen et al., 2006; Zhang et al., 2011);.

Fig. 5). The TOC value in Huangqihai obtained by this study shows a decrease trend since about 4500 cal. yr BP, later than other proxies (Fig. 5). Percentage of sands in Huangqihai obtained by this study had increased with great variations since about 4 cal. ka BP, in agreement with mean grain-size obtained by previous study (Zhang et al., 2011). We conservatively suggest that the local climate in Huangqihai had become drier and colder during 4 to 1 cal. ka BP (Fig. 5).

4.2. Response of forest development to climate drying

Our results showed that changes in vegetation types were relatively consistent with those reported by other studies in this region (Li et al., 2004; Wen et al., 2009; Zhao et al., 2009; Liu et al., 2010). During 9 to 7 cal. ka BP, the vegetation type was mainly *Pinus* forest and steppe, according to pollen evidence. Also, *Betula* and *Ulmus* were well developed in the study region, suggesting that the pioneer forests first occurring at the start of the Holocene had not disappeared (Liu et al., 2002). The pollen percentage of *Betula* even reached 15% in Anguli Nuur (Yin et al., 2011). Since 7 cal. ka BP, the percentage of arboreal pollen (AP) began to increase. Broadleaved trees were flourishing in these areas with increasing precipitation. Correspondingly, herbs, especially those indicating arid climate, declined substantially. This trend continued to about 4 cal. ka BP, consistent with the high values of Arboreal/Non-arboreal (AP/NAP) in Bayanchagan (Jiang et al., 2006). During 3.6 to 3.0 cal. ka BP, the pollen concentration reached its maximum. Hulun Nuur also displayed this obvious pollen concentration increase during 3 to 2 cal. ka BP, but the concentration change was not so remarkable as that at Huangqihai Lake (Fig. 6). During the following period, tree cover was low, indicating sparse tree coverage around Huangqihai Lake. Similar changes occurred in Hulun Nuur (Fig. 6). During the past 600 years, *Artemisia* and Chenopodiaceae have dominated the pollen record, which was consistent with most previous studies in the semi-arid region of China (e.g. Jiang et al., 2006; Liu et al., 2010).

There was a clear expansion of shrubs when the Asian monsoon weakened at about 3.6 cal. ka BP (A in Fig. 6). At present, shrublands occupy large areas of the mountains in North China (Wu, 1980; Kottek et al., 2006; Piao et al., 2009) and the distribution of shrublands has often been regarded as the result of either anthropogenic deforestation (Hannon et al., 2005) or climatic change (Archer, 2010). The shrubland has an advantage in barren soil when compared with forest or grassland, because shrub species are resistant to low available soil moisture in arid and semi-arid areas (Laliberte et al., 2004; Throop et al., 2012). Our results also showed that when the climate, especially the precipitation, was not suitable for forest growth, the shrub expanded into the forest regions while deforestation occurred. When the precipitation remained low for a long time, the shrubs were not competitive to grasses and the shrubland was finally replaced by steppe.

An alternative vegetation response was tree cover decline associated with the late Holocene drought, which occurred under prolonged drought conditions persisting for thousands of years (B in Fig. 6). In our study, we found a clear minimum in pollen concentration during 2970 to 600 cal. yr BP, suggesting low vegetation coverage. Drought can lead to decreasing available soil moisture, and a long period of low precipitation can reduce vegetation cover and enhance wind erosion of fine particles in soil. The coarsened soil was not conducive to soil water retention, further accelerating tree mortality and leading to forest fragmentation or "savannification", and an overall decrease in tree cover (Weltzin and McPherson, 1997). The soil particle sizes in our study have also shown that the sand content has increased markedly in the last 1500 years (Figs. 2, 4).

Either climatic or anthropogenic forcings could have contributed to the dominance of steppe during the last 600 years (C in Fig. 6). In our study, despite increases in the synanthropic species (including Chenopodiaceae and Asteraceae) after 1 cal. ka BP, there is still lack of other accurate evidence. The presence of these pollen grains was most likely caused by airborne pollen transport from deserts in the northwest

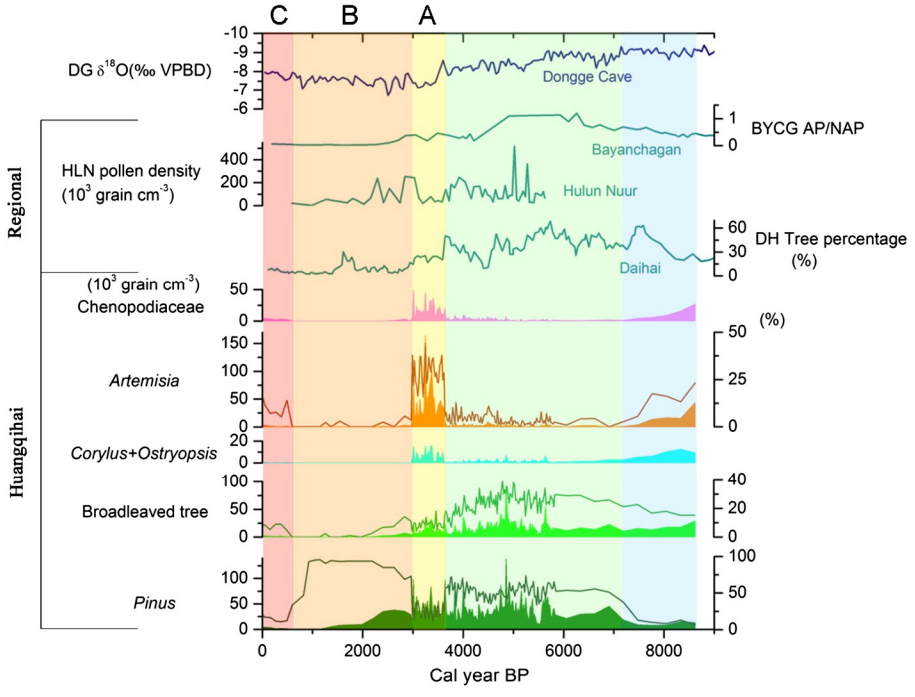

Fig. 6. Evolution of the terrestrial ecosystem in Huangqihai region over the past 8620 years, with rainfall changes based on stalagmite ^{18}O isotopes of Dongge Cave (Dykoski et al., 2005). Regional vegetation change: previous results from other lakes in the semi-arid region, pollen density of AP/NAP value of Bayanchagan (BYCG), pollen density of Hulun Nuur (HLN), and tree percentage of Daihai (DH) (Xiao et al., 2004; Jiang et al., 2006; Yin et al., 2013); Huangqihai vegetation change: the concentration and percentage of dominant pollen types, including major trees of *Pinus*, broadleaved trees, major shrubs of *Corylus* (+*Ostryopsis*), and major herbs of *Artemisia* and Chenopodiaceae. Three stages of vegetation responses to climatic drying are indicated as A: severe drought and shrub expansion in Huangqihai; B: long-term drought and savannification in Huangqihai; C: slight reversal of drought and grassland dominance in Huangqihai.

or by salty meadows dominated by *Sueda* species surrounding the water when the water level was sinking (Liu et al., 2008). According to the historical documents, agriculture activities began to increase 300 cal. yr BP, whereas human activity mainly consisted of moderate nomadic activities before that period (Yi, 2003; Zhang et al., 2007). Therefore, the human effects can be ignored and the increased herbaceous percentage was mainly an effect of decreased precipitation.

The inconsistency between monsoon development at a regional scale and vegetation responses at a local scale might also be associated with uncertainties in dating. In arid and semi-arid regions, the reservoir effect may yield dating ages that are 1000 to 2500 years older than the real age (Ren, 1998; Wu et al., 2007; Zhang et al., 2007). Since our calculated results were consistent with the abovementioned works, we reduced our core ages by 1440 years (Fig. 2). Following this adjustment, variations in pollen and sediment indexes were in better agreement with the grain-size change and magnetic susceptibility records for Huangqihai Lake (Shen et al., 2006; Zhang et al., 2011) and with changes in monsoon intensity (Dykoski et al., 2005). Although the reservoir effect will not have remained stable during the whole study period, we did not have further information regarding this correction, as is the case in other sediment sequences (Herzschuh et al., 2006). Therefore, we suggest that the main reason for the remaining inconsistency is that vegetation did not respond to monsoon development immediately. For example, when the precipitation changed, the forest might not have responded rapidly due to the long lifespan of trees.

5. Conclusions

We systematically reconstructed the Holocene climatic change and vegetation development in the Huangqihai Lake region, located in the forest-steppe ecotone in northern China. The Holocene climatic change captured in detail the regional-scale monsoon dynamics, especially the drying trend was obvious during 4 to 1 cal. ka BP. The corresponding vegetation dynamics were characterized by a steppe–forest–steppe sequence. Besides replacement of forest by steppe, we found two alternative responses of vegetation to drought: shrubland expansion and savannification. When the drying started, the shurbland began to expand into the forest when the Asian monsoon weakened at about 4 cal. ka BP. While the drought persisted for thousands of years, we found a clear minimum in vegetation coverage during 2970 to 600 cal. yr BP. The phenomenon that the forest did not respond rapidly to climate change might be explained by long lifespan of trees and the resistance of trees to environmental stress. Facing to future climate drought, the forest might not be replaced by steppe in a short time span.

Acknowledgements

This work was supported by the National Natural Science Foundation of China (NSFC grant numbers 41325002 and 31321061). We thank for Hu Guozheng, Qi Zhaohuan, Xu Xiaotian, Liu Guo and Wang Tao for their assistance in coring the lake sediment. We are also grateful to Dave Chandler for English editing.

References

Acácio, V., Holmgren, M., Rego, F., Moreira, F., Mohren, G.M., 2009. Are drought and wildfires turning Mediterranean cork oak forests into persistent shrublands? Agrofor. Syst. 76, 389–400.

Adams, H.D., Guardiola-Claramonte, M., Barron-Gafford, G.A., Villegas, J.C., Breshears, D.D., Zou, C.B., Troch, P.A., Huxman, T.E., 2009. Temperature sensitivity of drought-induced tree mortality portends increased regional die-off under global-change-type drought. Proc. Natl. Acad. Sci. 106, 7063–7066.

Allen, C.D., Macalady, A.K., Chenchouni, H., Bachelet, D., McDowell, N., Vennetier, M., Kitzberger, T., Rigling, A., Breshears, D.D., Hogg, E., 2010. A global overview of drought and heat-induced tree mortality reveals emerging climate change risks for forests. For. Ecol. Manag. 259, 660–684.

An, C.B., Feng, Z.D., Barton, L., 2006. Dry or humid? Mid-Holocene humidity changes in arid and semi-arid China. Quat. Sci. Rev. 25, 351–361.

An, C.B., Lu, Y., Zhao, J., Tao, S., Dong, W., Li, H., Jin, M., Wang, Z., 2012. A high-resolution record of Holocene environmental and climatic changes from Lake Balikun (Xinjiang, China): Implications for central Asia. The Holocene 22, 43–52.

Archer, S.R., 2010. Rangeland conservation and shrub encroachment: New perspectives on an old problem. Wild rangelands: Conserving wildlife while maintaining livestock in semi-arid ecosystems. 6, 53.

Battarbee, R.W., 2010. Aquatic ecosystem variability and climate change—A palaeoecological perspective. Clim. Change Impact Freshw. Ecosyst. 15–37.

Cai, Y., Zhang, M., Peng, Z., Lin, Y., An, Z., Zhang, Z., Cao, Y., 2001. The $\delta^{18}O$ variation of a stalagmite from Qixing Cave, Guizhou Province and indicated climate change during the Holocene. Chin. Sci. Bull. 46, 1904–1908.

Calvao, T., Palmeirim, J., 2004. Mapping Mediterranean scrub with satellite imagery: Biomass estimation and spectral behaviour. Int. J. Remote Sens. 25, 3113–3126.

Chen, F., Yu, Z., Yang, M., Ito, E., Wang, S., Madsen, D.B., Huang, X., Zhao, Y., Sato, T., John, B., Birks, H., 2008. Holocene moisture evolution in arid central Asia and its out-of-phase relationship with Asian monsoon history. Quat. Sci. Rev. 27, 351–364.

Clemens, S.C., Prell, W.L., Sun, Y., 2010. Orbital-scale timing and mechanisms driving Late Pleistocene Indo-Asian summer monsoons: Reinterpreting cave speleothem $\delta^{18}O$. Paleoceanography 25, PA4207.

De Deckker, P., Corrège, T., Head, J., 1991. Late Pleistocene record of cyclic eolian activity from tropical Australia suggesting the Younger Dryas is not an unusual climatic event. Geology 19, 602–605.

Dykoski, C.A., Edwards, R.L., Cheng, H., Yuan, D., Cai, Y., Zhang, M., Lin, Y., Qing, J., An, Z., Revenaugh, J., 2005. A high-resolution, absolute-dated Holocene and deglacial Asian monsoon record from Dongge Cave, China. Earth Planet. Sci. Lett. 233, 71–86.

Fleitmann, D., Burns, S.J., Mudelsee, M., Neff, U., Kramers, J., Mangini, A., Matter, A., 2003. Holocene forcing of the Indian monsoon recorded in a stalagmite from southern Oman. Science 300, 1737–1739.

Fleitmann, D., Burns, S.J., Mangini, A., Mudelsee, M., Kramers, J., Villa, I., Neff, U., Al-Subbary, A.A., Buettner, A., Hippler, D., 2007. Holocene ITCZ and Indian monsoon dynamics recorded in stalagmites from Oman and Yemen (Socotra). Quat. Sci. Rev. 26, 170–188.

Frelich, L.E., Reich, P.B., 2009. Will environmental changes reinforce the impact of global warming on the prairie-forest border of central North America? Front. Ecol. Environ. 8, 371–378.

Hannon, G.E., Bradshaw, R.H., Bradshaw, E.G., Snowball, I., Wastegård, S., 2005. Climate change and human settlement as drivers of late-Holocene vegetational change in the Faroe Islands. The Holocene 15, 639–647.

Herzschuh, U., 2007. Reliability of pollen ratios for environmental reconstructions on the Tibetan Plateau. J. Biogeogr. 34, 1265–1273.

Herzschuh, U., Winter, K., Wünnemann, B., Li, S., 2006. A general cooling trend on the central Tibetan Plateau throughout the Holocene recorded by the Lake Zigetang pollen spectra. Quat. Int. 154, 113–121.

Hu, C., Henderson, G.M., Huang, J., Xie, S., Sun, Y., Johnson, K.R., 2008. Quantification of Holocene Asian monsoon rainfall from spatially separated cave records. Earth Planet. Sci. Lett. 266, 221–232.

Huang, X., Chen, F., Fan, Y., Yang, M., 2009. Dry late-glacial and early Holocene climate in arid central Asia indicated by lithological and palynological evidence from Bosten Lake, China. Quat. Int. 194, 19–27.

Jiang, W., Guo, Z., Sun, X., Wu, H., Chu, G., Yuan, B., Hatté, C., Guiot, J., 2006. Reconstruction of climate and vegetation changes of Lake Bayanchagan (Inner Mongolia): Holocene variability of the East Asian monsoon. Quat. Res. 65, 411–420.

Kernan, M.R., Battarbee, R.W., Moss, B., 2010. Climate change impacts on freshwater ecosystems. Wiley Online Library.

Kottek, M., Grieser, J., Beck, C., Rudolf, B., Rubel, F., 2006. World map of the Koppen–Geiger climate classification updated. Meteorol. Z. 15, 259–264.

Laliberte, A.S., Rango, A., Havstad, K.M., Paris, J.F., Beck, R.F., McNeely, R., Gonzalez, A.L., 2004. Object-oriented image analysis for mapping shrub encroachment from 1937 to 2003 in southern New Mexico. Remote Sens. Environ. 93, 198–210.

Li, X., Zhou, J., Shen, J., Weng, C., Zhao, H., Sun, Q., 2004. Vegetation history and climatic variations during the last 14 ka BP inferred from a pollen record at Daihai Lake, north-central China. Rev. Palaeobot. Palynol. 132, 195–205.

Liu, H., Xu, L., Cui, H., 2002. Holocene history of desertification along the woodland–steppe border in northern China. Quat. Res. 57, 259–270.

Liu, H., Wei, F., Liu, K., Zhu, J., Wang, H., 2008. Determinants of pollen dispersal in the East Asian steppe at different spatial scales. Rev. Palaeobot. Palynol. 149, 219–228.

Liu, H., Yin, Y., Zhu, J., Zhao, F., Wang, H., 2010. How did the forest respond to Holocene climate drying at the forest-steppe ecotone in northern China? Quat. Int. 227, 46–52.

Liu, H., He, S., Anenkhonov, O., Hu, G., Sandanov, D., Badmaeva, N., 2012. Topography-controlled soil water content and the coexistence of forest and steppe in northern china. Phys. Geogr. 33, 561–573.

Liu, Z., Wen, X., Brady, E., Otto-Bliesner, B., Yu, G., Lu, H., Cheng, H., Wang, Y., Zheng, W., Ding, Y., 2014. Chinese cave records and the East Asia summer monsoon. Quat. Sci. Rev. 83, 115–128.

Maher, B.A., 2008. Holocene variability of the East Asian summer monsoon from Chinese cave records: A re-assessment. The Holocene 18, 861–866.

Maher Jr., L.J., Louis, J., 1981. Statistics for microfossil concentration measurements employing samples spiked with marker grains. Rev. Palaeobot. Palynol. 32, 153–191.

Moore, P.D., Webb, J.A., Collison, M., 1991. Pollen analysis. Blackwell Scientific Publications,.

O'Reilly, C.M., Alin, S.R., Plisnier, P.D., Cohen, A.S., McKee, B.A., 2003. Climate change decreases aquatic ecosystem productivity of Lake Tanganyika, Africa. Nature 424, 766–768.

Pausata, F.S., Battisti, D.S., Nisancioglu, K.H., Bitz, C.M., 2011. Chinese stalagmite $\delta^{18}O$ controlled by changes in the Indian monsoon during a simulated Heinrich event. Nat. Geosci. 4, 474–480.

Peng, C., Ma, Z., Lei, X., Zhu, Q., Chen, H., Wang, W., Liu, S., Li, W., Fang, X., Zhou, X., 2011. A drought-induced pervasive increase in tree mortality across Canada's boreal forests. Nat. Clim. Chang. 1, 467–471.
Piao, S., Fang, J., Ciais, P., Peylin, P., Huang, Y., Sitch, S., Wang, T., 2009. The carbon balance of terrestrial ecosystems in China. Nature 458, 1009–1013.
Porter, S.C., An, Z., 1995. Correlation between climate events in the North Atlantic and China during the last glaciation. Nature 375, 305–308.
Qiang, M., Chen, F., Zhang, J., Zu, R., Jin, M., Zhou, A., Xiao, S., 2007. Grain size in sediments from Lake Sugan: A possible linkage to dust storm events at the northern margin of the Qinghai–Tibetan Plateau. Environ. Geol. 51, 1229–1238.
Qiu, J., 2010. China drought highlights future climate threats. Nature 465, 142.
Reimer, P.J., Baillie, M.G., Bard, E., Bayliss, A., Beck, J.W., Bertrand, C.J., Blackwell, P.G., Buck, C.E., Burr, G.S., Cutler, K.B., 2004. IntCal04 terrestrial radiocarbon age calibration, 0–26 cal kyr BP. Radiocarbon 46, 1029–1058.
Ren, G., 1998. A finding of the influence of "Hard water" on radio carbon dating for lake sediments in Inner Mongolia, China. J. Lake Sci. 10 (3), 80–82 (in Chinese with English abstract).
Rosén, P., 2005. Total organic carbon (TOC) of lake water during the Holocene inferred from lake sediments and near-infrared spectroscopy (NIRS) in eight lakes from northern Sweden. Biogeochemistry 76, 503–516.
Rosén, P., Hammarlund, D., 2007. Effects of climate, fire and vegetation development on Holocene changes in total organic carbon concentration in three boreal forest lakes in northern Sweden. Biogeosciences 4, 975–984.
Shen, H., Jia, Y., Li, X., Wu, J., Wei, L., Wang, P., 2006. Environmental change inferred from distribution of Rb and Sr in different grain size fractions from lacustrine sediments in Huangqihai Lake, Inner Mongolia. Acta Geograph. Sin. 61 (11), 1208–1217 (in Chinese with English Abstract).
Sun, J., Li, S.-H., Han, P., Chen, Y., 2006. Holocene environmental changes in the central Inner Mongolia, based on single-aliquot-quartz optical dating and multi-proxy study of dune sands. Palaeogeogr. Palaeoclimatol. Palaeoecol. 233, 51–62.
Throop, H.L., Reichmann, L.G., Sala, O.E., Archer, S.R., 2012. Response of dominant grass and shrub species to water manipulation: An ecophysiological basis for shrub invasion in a Chihuahuan Desert Grassland. Oecologia 169, 373–383.
Van Mantgem, P.J., Stephenson, N.L., Byrne, J.C., Daniels, L.D., Franklin, J.F., Fulé, P.Z., Harmon, M.E., Larson, A.J., Smith, J.M., Taylor, A.H., 2009. Widespread increase of tree mortality rates in the western United States. Science 323, 521–524.
Wang, H., Liu, H., Zhu, J., Yin, Y., 2010. Holocene environmental changes as recorded by mineral magnetism of sediments from Anguli-nuur Lake, southeastern Inner Mongolia Plateau, China. Palaeogeogr. Palaeoclimatol. Palaeoecol. 285, 30–49.
Weltzin, J.F., McPherson, G.R., 1997. Spatial and temporal soil moisture resource partitioning by trees and grasses in a temperate savanna, Arizona, USA. Oecologia 112, 156–164.
Wen, R., Xiao, J., Chang, Z., Zhai, D., Xu, Q., Li, Y., Itoh, S., 2009. Holocene precipitation and temperature variations in the East Asian monsoonal margin from pollen data from Hulun Lake in northeastern Inner Mongolia, China. Boreas 39, 262–272.
Williams, J.W., Shuman, B., Bartlein, P.J., 2009. Rapid responses of the prairie–forest ecotone to early Holocene aridity in mid-continental North America. Glob. Planet. Chang. 66, 195–207.
Wu, Z., 1980. Vegetation of China. Science, Beijing.
Wu, Y., Lücke, A., Zhangdong, J., Sumin, W., Schleser, G.H., Battarbee, R.W., Weilan, X., 2006. Holocene climate development on the central Tibetan Plateau: A sedimentary record from Cuoe Lake. Palaeogeogr. Palaeoclimatol. Palaeoecol. 234, 328–340.
Wu, Y., Wang, S., Zhou, L., Sun, Z., 2007. Modern reservoir age for 14C dating in Daihai. Quat. Sci. 27 (4), 507–510 (in Chinese with English abstract).
Wu, J., Wang, Y., Dong, J., 2011. Changes in East Asia summer monsoon during the Holocene recorded by stalagmite $\delta^{18}O$ records from Liaoning Province. Quat. Sci. 31 (6), 990–998 (in Chinese with English abstract).
Xiao, J., Xu, Q., Nakamura, T., Yang, X., Liang, W., Inouchi, Y., 2004. Holocene vegetation variation in the Daihai Lake region of north–central China: A direct indication of the Asian monsoon climatic history. Quat. Sci. Rev. 23, 1669–1679.
Xiao, J., Wu, J., Si, B., Liang, W., Nakamura, T., Liu, B., Inouchi, Y., 2006. Holocene climate changes in the monsoon/arid transition reflected by carbon concentration in Daihai Lake of Inner Mongolia. The Holocene 16, 551–560.
Yang, L., Zhou, J., Lai, Z., Long, H., Zhang, J., 2010. Late glacial and Holocene dune evolution in the Horqin dunefield of northeastern China based on luminescence dating. Palaeogeogr. Palaeoclimatol. Palaeoecol. 296, 44–51.
Yi, B., 2003. Northeast grassland development and the ecological cost since the Qing Dynasty. Agric. Hist. China 4, 116 (in Chinese).
Yin, Y., Liu, H., He, S., Zhao, F., Zhu, J., Wang, H., Liu, G., Wu, X., 2011. Patterns of local and regional grain size distribution and their application to Holocene climate reconstruction in semi-arid Inner Mongolia, China. Palaeogeogr. Palaeoclimatol. Palaeoecol. 307, 168–176.
Yin, Y., Liu, H., Liu, G., Hao, Q., Wang, H., 2013. Vegetation responses to mid-Holocene extreme drought events and subsequent long-term drought on the southeastern Inner Mongolian Plateau, China. Agric. For. Meteorol. 178–179, 3–9.
Zhai, Q., Guo, Z., Li, Y., Li, R., 2006. Annually laminated lake sediments and environmental changes in Bashang Plateau, North China. Palaeogeogr. Palaeoclimatol. Palaeoecol. 241, 95–102.
Zhang, M.A., Borjigin, E., Zhang, H., 2007. Mongolian nomadic culture and ecological culture: On the ecological reconstruction in the agro-pastoral mosaic zone in Northern China. Ecol. Econ. 62, 19–26.
Zhang, J., Jia, Y., Lai, Z., Long, H., Yang, L., 2011. Holocene evolution of Huangqihai Lake in semi-arid northern China based on sedimentology and luminescence dating. The Holocene 21, 1261–1268.
Zhao, Y., Yu, Z., Chen, F., Ito, E., Zhao, C., 2007. Holocene vegetation and climate history at Hurleg Lake in the Qaidam Basin, northwest China. Rev. Palaeobot. Palynol. 145, 275–288.
Zhao, Y., Yu, Z., Chen, F., 2009. Spatial and temporal patterns of Holocene vegetation and climate changes in arid and semi-arid China. Quat. Int. 194, 6–18.
Zhao, Y., Liu, H., Li, F., Huang, X., Sun, J., Zhao, W., Herzschuh, U., Tang, Y., 2012. Application and limitations of the Artemisia/Chenopodiaceae pollen ratio in arid and semi-arid China. The Holocene 22, 1385–1392.
Zhou, Y., Lu, H., Joseph, M., Miao, X., James, S., Ronald, G., 2008. Optically stimulated luminescence dating of aeolian sand in the Otindag dune field and Holocene climate change. Sci. China Ser. D Earth Sci. 51, 837–847.